ORGANIC PROCESS RESEARCH & DEVELOPMENT
OPR&D

pubs.acs.org/OPRD

Article

Development of a Robust Manufacturing Route for Molnupiravir, an Antiviral for the Treatment of COVID-19

Patrick S. Fier,* Yingju Xu,* Marc Poirier, Gilmar Brito, Michelle Zheng, Rachel Bade, Eric Sirota, Kevin Stone, Lushi Tan, Guy R. Humphrey, Darryl Chang, Jameson Bothe, Yongqian Zhang, Frank Bernardoni, Steve Castro, Michael A. Zompa, Jerry Taylor, Kevin M. Sirk, Anthony Diaz-Santana, Ike Diribe, Khateeta M. Emerson, Bharath Krishnamurthi, Ralph Zhao, Michael Ward, Chengqian Xiao, Honggui Ouyand, Jianfeng Zhan, and William J. Morris

Cite This: *Org. Process Res. Dev.* 2021, 25, 2806–2815

Read Online

ACCESS | Metrics & More | Article Recommendations | Supporting Information

ABSTRACT: Herein is described the development of a large-scale manufacturing process for molnupiravir, an orally dosed antiviral that was recently demonstrated to be efficacious for the treatment of patients with COVID-19. The yield, robustness, and efficiency of each of the five steps were improved, ultimately culminating in a 1.6-fold improvement in overall yield and a dramatic increase in the overall throughput compared to the baseline process.

KEYWORDS: *molnupiravir, covid-19, antiviral, crystallization*

Molnupiravir (MK-4482, formerly EIDD-2801; Figure 1A)[1] is an orally dosed unnatural nucleoside prodrug that has demonstrated antiviral activity in preclinical studies[2−4] and was recently shown to significantly reduce the rate of hospitalization and death in patients diagnosed with COVID-19.[5] In vivo, molnupiravir undergoes ester cleavage to reveal *N*-hydroxycytidine, followed by subsequent reactions to form the active triphosphate species (Figure 1A). The proposed mechanism of antiviral activity is through tautomerization of the *N*-hydroxycytosine base, with the two tautomers mimicking either uridine or cytidine, which ultimately leads to viral error catastrophe during RNA replication (Figure 1B).[6]

In May of 2020, Merck & Co., Inc., Kenilworth, NJ, USA announced a partnership with Ridgeback Biotherapeutics to further advance molnupiravir in clinical trials.[1] Given the projected high demand for an orally dosed small molecule therapeutic for COVID-19, a robust and efficient manufacturing route was required that could produce this compound in quantities over 100 metric tons per year.[7] While the existing five-step synthesis from uridine (Scheme 1), developed by Ridgeback and Olon Ricerca, was demonstrated to produce high-purity API on lab and pilot scale, several low-yielding steps, lengthy operations, and robustness concerns prompted us to optimize each step to enable large-scale manufacturing to supply molnupiravir across the world. Herein, we report the process optimization for each of the five steps which were realized over the course of just a few months during the global pandemic, ultimately culminating in a 1.6-fold improvement in overall yield, much improved robustness, and significant reductions in cycle times and waste generation.

The first step in the synthesis of molnupiravir is the protection of the two secondary alcohols of uridine as an acetonide (Scheme 2).[8] In the original process, installation of the protecting group was carried out with 2,2-dimethoxypropane (DMP) with catalytic H_2SO_4 in acetone (8 L/kg) at reflux, with the liberation of two equivalents of methanol. At the end of the reaction, the mixture was neutralized at elevated temperature with Et_3N, and the product was allowed to crystallize by cooling to 0−5 °C and then isolated via filtration. This reaction would reliably and rapidly reach 95−96% conversion and provide acetonide **1** in yields of 70−75% due to high losses in the mother liquor. It was deemed critical to improve the throughput and to increase conversion of uridine to greater than 99% because uridine has low solubility and would cocrystallize with **1**, resulting in up to 5% of uridine in the isolated solid.

Initially, an exploration of alternate reaction solvents and acids was investigated to improve conversion and recovery. While numerous combinations of solvents and acids could be used for this transformation, many resulted in thick reaction mixtures that could not be easily agitated, modest reaction rates, and/or high losses in the supernatant. Ultimately, acetone was maintained as the reaction solvent, as it provided reliably fast reaction rates and easily agitable slurries. The solvent volume was reduced from 8 to 5 L/kg to maximize volumetric efficiency while still affording easily managed slurries. In a typical experiment carried out near reflux, 95% conversion of uridine to acetonide **1** occurs within minutes with only 1 mol % H_2SO_4 and 1.05 equiv of DMP. While the

Received: October 25, 2021
Published: December 10, 2021

https://doi.org/10.1021/acs.oprd.1c00400
Org. Process Res. Dev. 2021, 25, 2806–2815

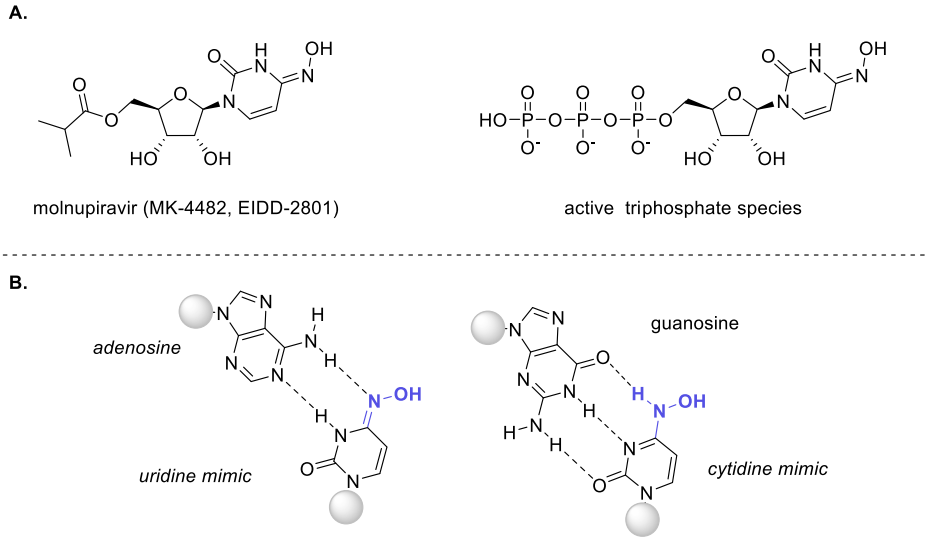

Figure 1. (A): Structure of molnupiravir and in vivo formed triphosphate species. (B): Proposed mechanism of action involving tautomerization and different base-pairing interactions at RNA polymerase. Gray circles represent ribosyl subunits.

Scheme 1. Summary of the Process for the Synthesis of Molnupiravir from Uridine

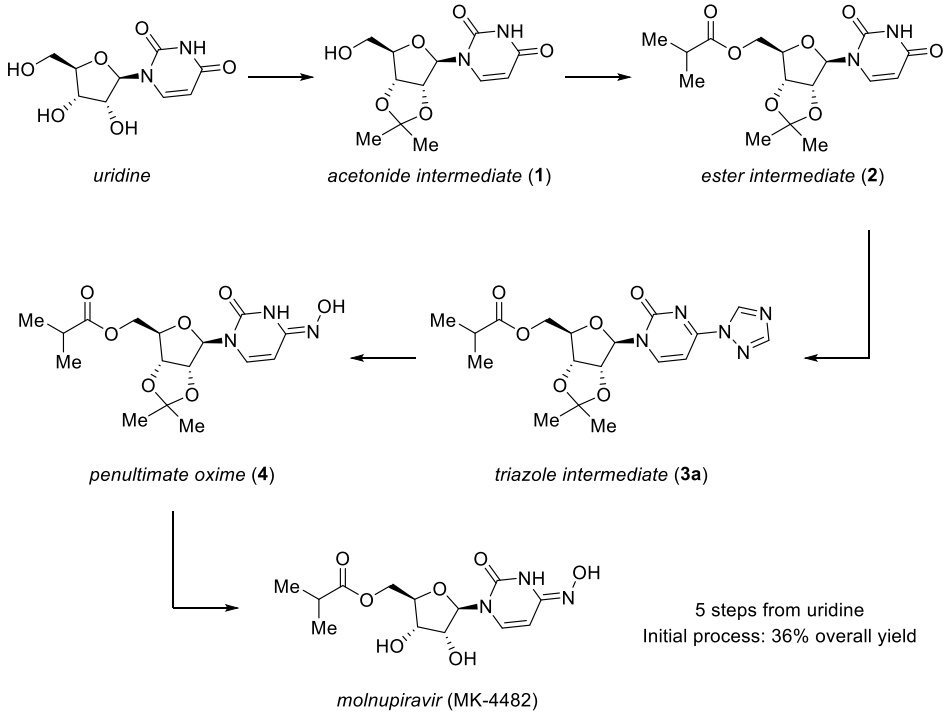

Scheme 2. Original Process for the Synthesis of Acetonide Intermediate 1

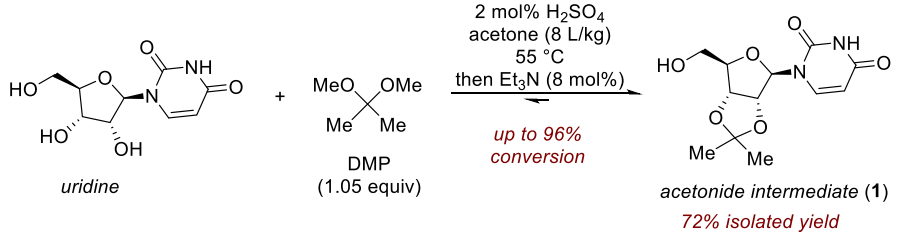

reaction can occur at lower temperatures, including ambient temperature, carrying out the reaction at reflux provided reliable and well-controlled reaction mixtures and avoided thick or unstirrable slurry-to-slurry transformations and risks of uridine entrainment in the solid. Notably, the addition of a larger excess of DMP did not significantly impact the reaction

https://doi.org/10.1021/acs.oprd.1c00400
Org. Process Res. Dev. 2021, 25, 2806−2815

Scheme 3. Final Process for the Synthesis of Acetonide Intermediate 1 with Temperature-Induced Dynamic Crystallization and *n*-Heptane Addition to Improve Recovery

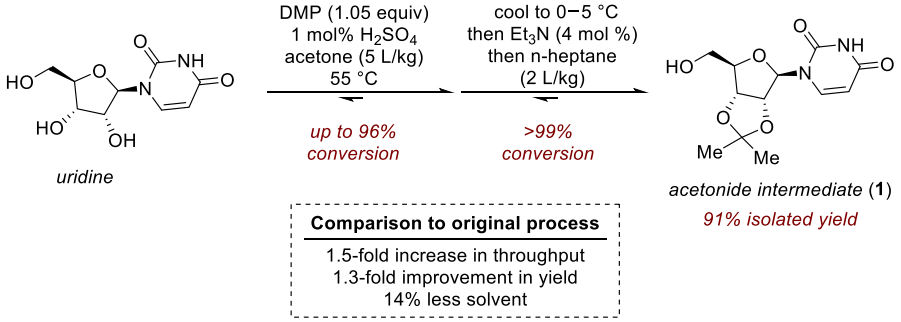

Scheme 4. Comparison of the Original and Final Processes for the Preparation of the Ester Intermediate 2

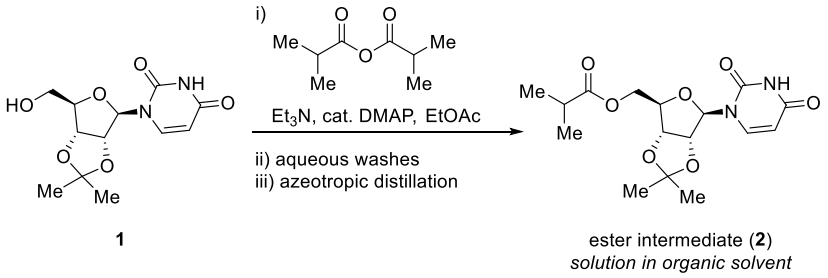

Parameter	Original process	Improved process
EtOAc	8 L/kg	5 L/kg
Isobutyric acid	1.22 equiv	1.1 equiv
Et_3N	2.5 equiv	1.5 equiv
DMAP	5 mol%	2 mol%
Washes	water then brine, ca. 5% loss	water, ca. 2% loss
Isolation solvent	EtOAc; **2** poorly soluble	MeCN; **2** highly soluble

conversion but did negatively impact reaction purity through the formation of bis-ketal and dimeric impurities.

The incomplete conversion observed with excess DMP is consistent with the reaction being in equilibrium and exhibiting a thermodynamic ratio of approximately 96:4 **1**:uridine at 55 °C in acetone. Testing the reverse reaction by subjecting pure **1** to 2 equiv of methanol and 1 mol % H_2SO_4 in acetone formed the same ratio of uridine and **1**, further confirming the equilibrium nature of the reaction. As mentioned above, it was necessary to further increase the conversion in order to prevent cocrystallization of uridine with **1**, as uridine-derived products would form and persist in downstream reactions. With the fast rate of the forward and reverse reactions, it was envisioned that maintaining the high solution equilibrium of the product while selectively crystallizing the product (dynamic crystallization) could drive the reaction to complete conversion. Indeed, a dynamic crystallization could be achieved by either adding antisolvent (*n*-heptane) to the reaction mixture and/or cooling the reaction. In these experiments, the conversion to **1** could be increased to >99%, improving the yield and avoiding cocrystallization of **1** with unreacted uridine.

The reaction and isolation conditions were further refined to arrive at the final commercial process (Scheme 3). The process involves an initial heat up to approximately 55 °C to form approximately 95% **1**, and this mixture is then cooled to 0−5 °C to perform the dynamic crystallization and increase conversion to >99%, after which the mixture is quenched with Et_3N to halt the reaction. At this stage, there is approximately 20% of the product still in solution, which can be decreased significantly by the addition of heptane (2 L/kg) without impacting purity. Acetonide product **1** prepared this way provides an average isolated yield of 91% and HPLC purity greater than 99.5% on a metric ton scale. Without the dynamic crystallization procedure, controlling the residual uridine was not possible without incurring significant losses, and the uridine-derived impurities would persist throughout the rest of the synthesis. Compared to the original process, the changes described here improved the yield by 1.3-fold and resulted in 14% less solvent use. Taken together, these improvements provide a 1.5-fold improvement in material throughput for a given reactor.

Next, the 5′ isobutyrate group is installed on intermediate **1** with isobutyric anhydride, Et_3N, and catalytic DMAP to afford the ester intermediate **2**. The initial reaction conditions gave >99% conversion to product in high purity, and the product was through-processed as an approximately 30 wt % solution in ethyl acetate after two aqueous washes and azeotropic drying. We aimed to maximize volumetric productivity and decrease losses during the aqueous workup (ca. 5%) while ensuring high purity of **2**. Notably, the product was prone to crystallization upon storage as a solution in EtOAc, which was flagged as a significant risk for large-scale manufacturing.

With high-yielding reaction conditions from the outset, we opted to decrease the amount of solvent in the reaction from 8 to 5 L/kg, while also decreasing the charges of Et_3N, DMAP,

https://doi.org/10.1021/acs.oprd.1c00400
Org. Process Res. Dev. 2021, 25, 2806−2815

Scheme 5. (A) Original Reaction and Isolation Conditions for Triazole Intermediate 3a. (B) Primary Side Products Observed during the Reaction

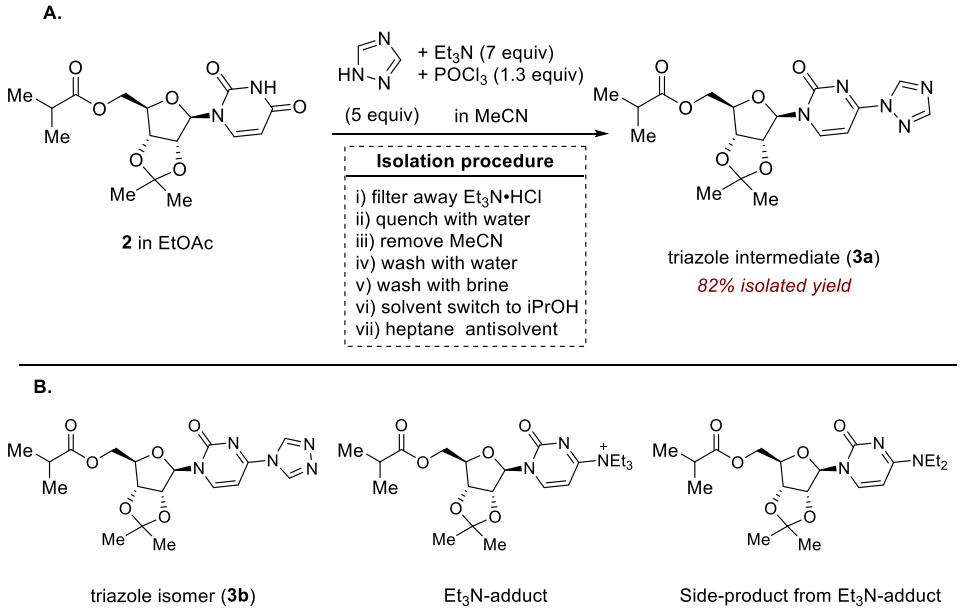

Scheme 6. Final Reaction and Isolation Conditions to Prepare Triazole Intermediate 3a[a]

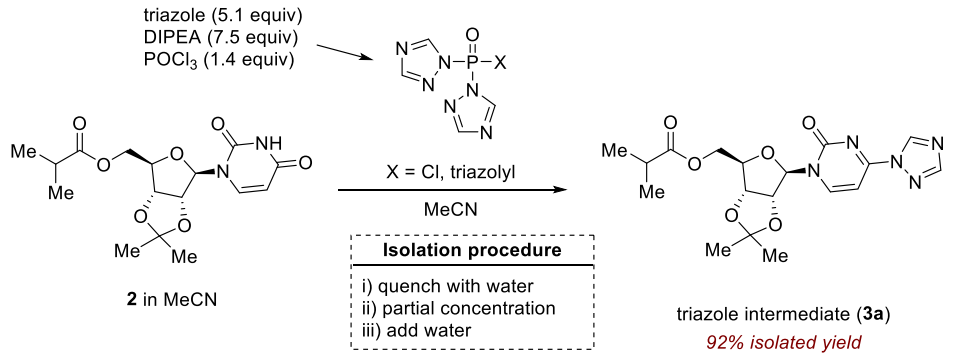

[a]See Supporting Information for additional details.

and isobutyric anhydride (Scheme 4). The aqueous workup was modified to a single 2 L/kg water wash, resulting in less than 2% loss to the aqueous layer. Spiking experiments demonstrated that residual isobutyric acid and Et_3N had no impact on the stability of the through-processed solution of intermediate **2** or in the performance of step 3, so additional water washes to remove all of the isobutyric acid and Et_3N were not performed. Finally, the EtOAc solution was azeotropically dried and solvent switched to MeCN (target water content below 0.1 wt %) to provide the final solution of **2** that is directly used in the third step. Intermediate **2** exhibits much greater solubility in MeCN (>50 wt % at 20 °C) compared to EtOAc (ca. 25 wt % at 20 °C) and does not pose a risk of precipitation upon storage. Furthermore, MeCN is the solvent used in the subsequent step, and through-processing **2** in MeCN instead of EtOAc also provided slight improvements to the reaction rates in step 3. Overall, the esterification reaction reliably provides intermediate **2** in >98% yield on a metric ton scale with no side products derived from **1**. Notably, the process changes avoid unnecessary waste generation and resulted in a 1.5-fold improvement in overall productivity.

The third step towards molnupiravir is activation of the amidic carbonyl on the uracil ring and substitution with 1,2,4-triazole to form the triazole intermediate **3a**.[9] The initial process involved the in situ formation of a triazole phosphate reagent with 1,2,4-triazole, Et_3N, and $POCl_3$ in acetonitrile, followed by addition of the intermediate **2** solution. The formation of the triazole phosphate reagent is rapid and generates a thick slurry of Et_3N·HCl, and this thick slurry was identified as a potential risk for large-scale manufacturing. Reaction of the in situ formed reagent with intermediate **2** occurred with >98% conversion over the course of 18−24 h at ambient temperature; however, 5−8% of the Et_3N adduct (Scheme 5) was formed as a byproduct. This adduct did not significantly convert to the desired product with extended aging, but rather formed the diethylamine adduct via loss of an ethyl group. Finally, the product was isolated after filtration of the Et_3N·HCl salts, a solvent switch to EtOAc, aqueous workup, a second solvent switch and azeotropic drying with IPA, and finally crystallization with heptane. While suitable for initial scale up, given the projected demands of molnupiravir, the isolation alone would result in several million kilograms of

https://doi.org/10.1021/acs.oprd.1c00400
Org. Process Res. Dev. 2021, 25, 2806−2815

Scheme 7. (A) Comparison of the Original and Improved Processes. (B) Major Impurities Formed during the Reaction

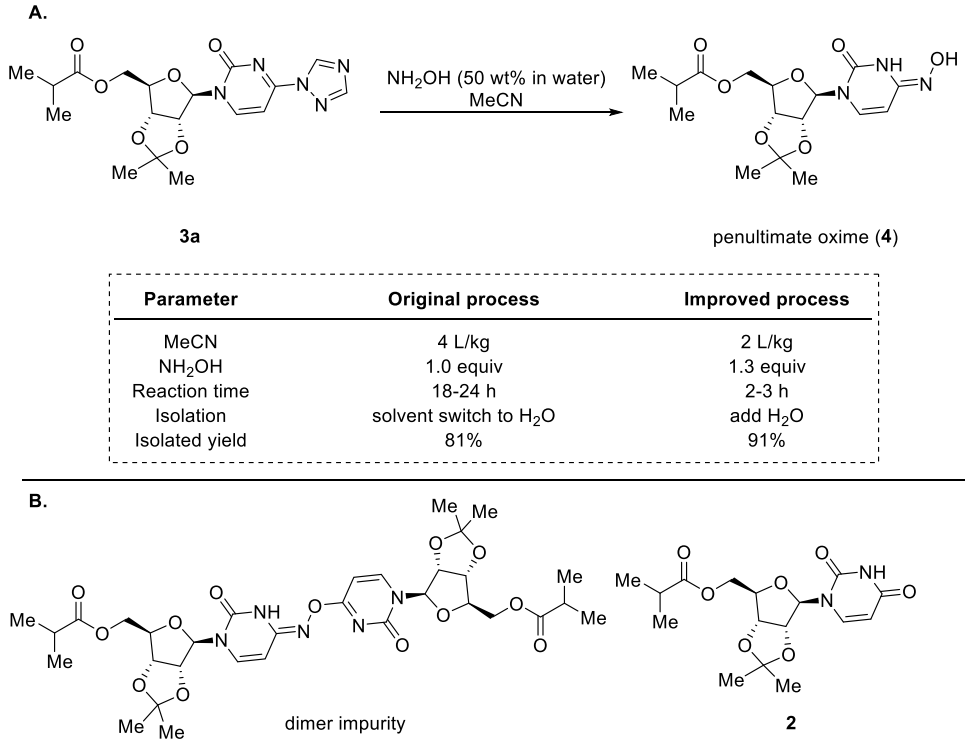

Parameter	Original process	Improved process
MeCN	4 L/kg	2 L/kg
NH_2OH	1.0 equiv	1.3 equiv
Reaction time	18-24 h	2-3 h
Isolation	solvent switch to H_2O	add H_2O
Isolated yield	81%	91%

organic solvent waste each year and required approximately 10 days to execute at manufacturing scale.

To avoid the thick reaction slurry due to $Et_3N{\cdot}HCl$ salts, the Et_3N adduct side products, and the filtration of salts during isolation, the base was changed to diisopropylethylamine (DIPEA, Hunig's base). With this change (Scheme 6), the entire reaction sequence was homogeneous, and no amine adduct impurities were formed, enabling formation of the product in nearly quantitative assay yield. The reaction of the triazole phosphate reagent with **2** is fast, often reaching >98% conversion within 1 h to a mixture of two products (**3a** and **3b**). As 1,2,4-triazole is nucleophilic at both the N1/N2 and N4 positions, during the course of the reaction, a mixture of the desired product **3a** and the isomeric product **3b** are formed. At early time points, the ratio is approximately 85:15 **3a**:**3b** and increases over the course of several hours to form thermodynamically more stable **3a** in a greater than 99:1 ratio. Conversion of the isomer **3b** to **3a** requires free 1,2,4-triazole, and its rate was qualitatively found to be dependent on the amount of free triazole available, leading to the selection of reaction conditions with a 3.6:1 ratio of triazole/$POCl_3$. A slight excess of $POCl_3$ (1.4 equiv) was required to ensure high conversion of **2** in the presence of adventitious water present in the raw materials and solvents.

Given the large amounts of solvent waste, energy usage, and long cycle times in the existing isolation, we explored options to directly crystallize **3a** from the reaction mixture. As the byproducts and reagents used in the reaction are all highly water soluble and **3a** is poorly water soluble, a direct crystallization with water as the antisolvent was developed. After reaction completion, the mixture is quenched with 1 L/kg of water to ensure hydrolysis of any reactive phosphate species, followed by a partial concentration to remove the majority of MeCN. During the concentration, a portion of the product crystallizes out of solution, and it was found that this uncontrolled crystallization could lead to entrapment of DIPEA and its salts in the solid. Thus, after the initial water addition and concentration, the slurry is heated at 40 °C to ensure dissolution of any entrapped material, after which water is added in a controlled fashion to generate crystalline **3a**. Cooling to 7 °C minimizes losses while ensuring complete solubility of all other components, and the product is filtered and washed with water. The reaction and isolation sequence described here provides an average of 92% isolated yield, >99.5 HPLC purity, and >99 wt % purity on a metric ton scale and avoids the use of excessive organic solvents and unit operations for the isolation. Compared to the original process, the yield was improved by 10%, and the cycle time shortened by several days per batch. With the anticipated large volumes of molnupiravir, the green chemistry improvements are particularly noteworthy. In fact, for every 100 metric tons of molnupiravir produced, the improved isolation process described here will avoid over 8 million kg of organic solvent waste that would have been used with the original isolation sequence.

Several process safety issues are worth mentioning[10] for this step: (1) 1,2,4-triazole is known to be a highly energetic compound with an exotherm onset around 280 °C and 1700 J/g under DSC (differential scanning calorimeter) at a 10 °C/min scan rate in a high pressure gold-plated test cell. However, drop weight testing showed its negative impact at an impact energy level of 50 J. (2) DSC testing of the in situ formed triazole phosphate mixture showed an exotherm of 63 J/g (onset near 123 °C) and 36 J/g (onset near 322 °C) with DIPEA as the base (homogeneous) versus an exotherm of 63 J/g (onset ~73 °C) and >205 J/g (onset ~299 °C). While both are acceptable in terms of a safety basis, the overall safety profile was improved by using DIPEA as the base due to a higher onset temperature of the first exotherm (higher than the bp of the solvent). (3) The triazole intermediate **3a** showed an

https://doi.org/10.1021/acs.oprd.1c00400
Org. Process Res. Dev. 2021, 25, 2806−2815

Scheme 8. (A) Comparison of the Original and Improved Reaction Conditions. (B) Major Impurities Present at the End of the Reaction: (C) Comparison of Workup and Isolation Conditions

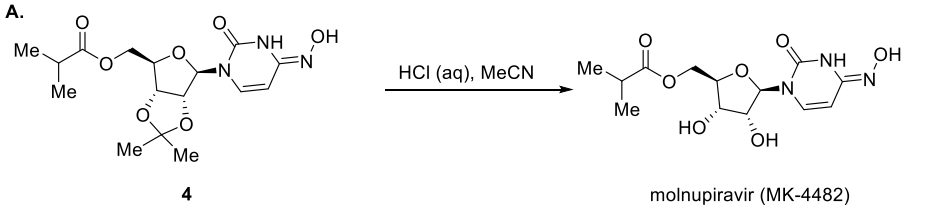

Reaction parameter	Original process	Improved process
HCl	2 M, 0.76 equiv	5.3 M, 0.85 equiv
MeCN	8 L/kg	8 L/kg
Temp. and time	56 °C, 18 h	60 °C, 12 h

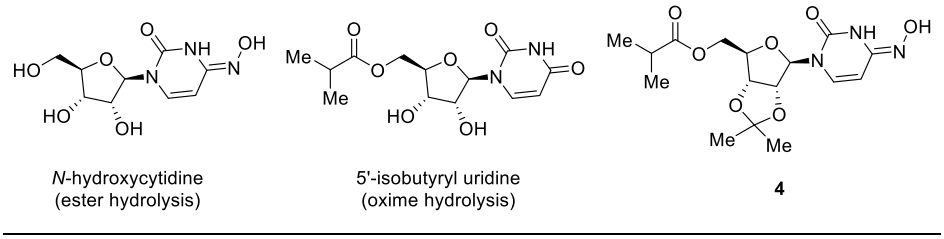

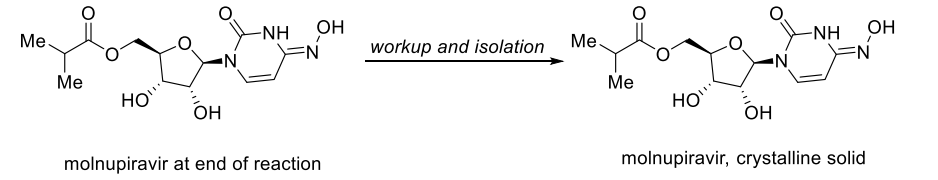

Isolation parameter	Original process	Improved process
Base to neutralize H_2O present after quench	5.3 wt% $NaHCO_3$ ca. 4 L/kg	13.1 wt% Na_2CO_3 ca. 1 L/kg
Extraction procedures	i) Back extractions from water ii) water wash of EtOAc layers	i) wash with Na_2SO_4/Na_2EDTA ii) wash with minimal water
Crystallization procedure	Azeotropic drying with EtOAc; crystallization during distillation	Azeotropic drying with EtOAc; crystallization during EtOAc addition

exotherm of 570 J/g with an onset of 268 °C. The concentration before the final isolation does not show any significant exotherm up to 400 °C on DSC. (4) Reaction calorimetry showed that dosing $POCl_3$ is highly exothermic with DT adiabatic of 53 K with DIPEA as the base versus 68 K with TEA as the base, both instantaneous with no heat accumulation. (5) Dosing intermediate **2** is less exothermic with DT adiabatic around 20−30 K with 10−15% heat accumulation right after dosing. (6) Quenching $POCl_3$ has caused numerous lab and plant accidents due to quenching temperatures being set too low which does not immediately initiate the reaction of water with $POCl_3$. Thus, the water quenching temperature was purposely set to above ambient temperature.

The preparation of penultimate oxime **4** is achieved by displacement of the triazole group in **3a** with aqueous NH_2OH (Scheme 7).[11] Initial conditions used 1.0 equiv of NH_2OH with 4 L/kg MeCN and isolated the product after a solvent switch to water. The use of an equimolar amount of NH_2OH not only resulted in slow reaction rates (>18 h) but also resulted in the potential for incomplete conversion due to variability in the concentration of aqueous NH_2OH and charging tolerances. In addition, a dimeric impurity (Scheme 7B) was formed in significant levels and was poorly rejected during the crystallization. The dimeric impurity could be removed during isolation by washing the cake with MTBE; however, this was not considered to be a robust control strategy and also resulted in high product losses.

To circumvent these issues, we opted to increase the charge of NH_2OH to 1.3 equiv while also maximizing the reaction concentration at just 2 L/kg MeCN. Under these reaction conditions, complete conversion of **3a** is achieved in just 2−3 h. During the course of the reaction, approximately 5% of triazole **3** reverts to intermediate **2**; however. this side product is well-rejected in the crystallization and isolation of **4**. The dimeric impurity, noted above, is observed at early time points

https://doi.org/10.1021/acs.oprd.1c00400
Org. Process Res. Dev. 2021, 25, 2806−2815

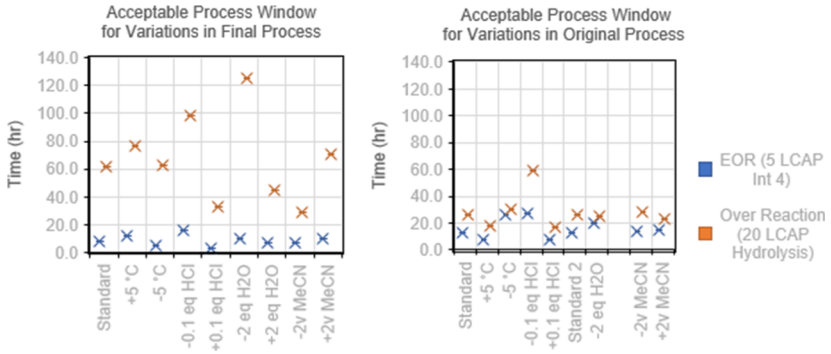

Figure 2. Comparison of robustness via an acceptable process window for original and final sets of process conditions in consideration for the API-forming reaction, both leading to high-quality API under "standard" conditions yet with vast differences in operational flexibility. EOR = end of reaction.

but is converted to the desired product over the course of the reaction due to the higher concentration of NH_2OH compared to the initial conditions. The distillation of aqueous hydroxylamine is known to be dangerous, and thus, avoiding a distillation was deemed to be a necessary practice.[12] By running the reaction at higher concentration, the product can be crystallized directly by the addition of water, avoiding the solvent switch employed in the initial isolation and safety concerns with generating NH_2OH vapors. These improvements not only simplify the isolation and ensure high purity of penultimate oxime **4** but also provide the product in 10% higher yield compared to the original process (91 vs 81% isolated yield).

Completion of the synthesis of molnupiravir involves removal of the acetonide protecting group under acidic conditions (Scheme 8).[8] While the acid-catalyzed deprotection of acetonides is commonplace, molnupiravir contains acid-sensitive ester and oxime functional groups that are prone to hydrolysis. The initial reaction conditions employed 2 M aqueous HCl in acetonitrile at 56 °C and achieved approximately 95% conversion over 16 h, typically with the formation of over 10% of *N*-hydroxycytidine (ester hydrolysis) and 3−5% of 5′-isobutyryl uridine (oxime hydrolysis) byproducts. The reaction was also found to be extremely sensitive to the amount of acid charged and reaction temperature, with subtle changes in either variable resulting in significant rate and purity profile differences compared to the control. After reaction completion, the amount of the over-hydrolysis byproducts increased significantly and required the reaction to be quenched immediately to ensure quality API could be isolated. Given the sensitivities with the charges, reaction times, and impurity generation, the identification of more robust and reproducible reaction conditions was essential in order to ensure the supply of high purity molnupiravir on a multimetric ton scale in high yield. Equally important was the observation that, upon neutralizing the reaction, a deep purple color appeared which persisted over the course of the workup and crystallization, presenting a risk of forming purple-colored API.

To optimize the reaction conditions, a series of high-throughput screens was carried out with automated sampling to collect data on the kinetics of product and impurity formation. A broad exploration of four process variables (HCl, water, MeCN, and temperature) revealed interacting and nonlinear relationships attributed to the nature of the acidic, biphasic mixtures and the hydrolysis kinetics to related impurities. It was found that relatively minor changes to these process factors could lead to the presence of these impurities as primary products in this exceptionally sensitive system. Following traditional development heuristics in the same rapid pace of automated parallel experimentation, two potential operating conditions were identified at distinctly distant local optima in the parameter space. The speed of automation enabled a full kinetic characterization of both processes for an evaluation of robustness via an "acceptable process window"—the length of time over which a varied process will result in material of known, acceptable quality at end-of-reaction. This analysis revealed a 5-fold improvement in robustness for one process over the other, despite the surface-level similarity of each target condition's performance (Figure 2).

The final reaction conditions use 0.85 equiv of concentrated HCl, 5 equiv of water, 8 L/kg MeCN as the reaction solvent, and aging at 60 °C for approximately 12 h. After 12 h, the reaction mixture can be cooled to ambient temperature for sampling without concern for byproduct formation while awaiting results to confirm that the reaction reached the target of at least 95% conversion. These conditions also minimized byproduct formation during the aging at 60 °C and could provide quality API even with extended aging. In a typical experiment, the assay yield of molnupiravir is greater than 85% with reproducible levels of *N*-hydroxycytidine, 5′-isobutyryl uridine, and residual penultimate **4**.

With reaction conditions in hand, we worked to ensure that the workup and crystallization were equally robust. In the original process, the reaction was neutralized with 5.3 wt % aqueous $NaHCO_3$, followed by a solvent switch to EtOAc, back extractions of the aqueous layer, a single water wash of the combined organic layers, and finally azeotropic distillation and the addition of MTBE to form the crystalline API. To improve the isolation, we wanted to avoid the significant off-gassing from sodium bicarbonate, minimize the introduction of water (>3 L/kg water from $NaHCO_3$) to circumvent the back extractions, ensure remediation of the purple color (vide supra) that was often observed, and develop a more controlled crystallization.

Each of the workup and isolation inefficiencies and risks were addressed by modifying the reagents and operations. First, the aqueous base used in the quench was changed from 5.3 wt % $NaHCO_3$ to 13.2 wt % Na_2CO_3. The change to Na_2CO_3 avoided the significant off-gassing that was observed with $NaHCO_3$ and introduced less than one-third the amount

https://doi.org/10.1021/acs.oprd.1c00400
Org. Process Res. Dev. 2021, 25, 2806−2815

Scheme 9. Summary of Process Improvements to Prepare Molnupiravir from Uridine

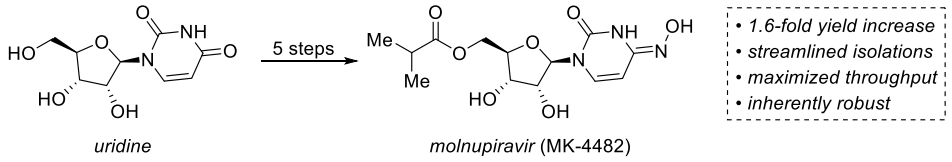

of water which was necessary to avoid the tedious back extractions. The purple color noted above was present after neutralization and throughout the solvent switch and was only partially removed through standard aqueous washes. To ensure the isolation of colorless API, we investigated the root cause of the color and identified that it was due to trace levels of iron (color observed in isolated solid above ca. 30 ppm Fe) that were introduced from raw materials or equipment. Knowing the source of the color, we found that iron could be completely sequestered from the API by incorporating Na_2EDTA in the first aqueous wash. In practice, after the solvent switch, the organic phase is washed with 2 L/kg of a solution comprising 15 wt % Na_2SO_4 and 1 wt % $Na_2EDTA{\cdot}2H_2O$. The high concentration of Na_2SO_4 also removes residual water that was introduced from the sodium carbonate quench, extracts a portion of the *N*-hydroxycytidine byproduct, and prevents product loss to this initial aqueous wash. The choice of 15 wt % sodium sulfate was selected to balance product losses to the aqueous while also preventing solids from forming in the aqueous layer or at the interface. The amount of EDTA ensures rapid and complete removal of iron and prevents iron complexes with the API, resulting in a colorless organic phase and derisking the formation of colored API. The organic layer is then washed with a minimum amount of water (0.75 L/kg) to remove trace inorganic salts and most of the residual *N*-hydroxycytidine byproduct.

The EtOAc solution that remains contains approximately 5.5 wt % water and 55 mg/mL concentration of molnupiravir. The solubility of molnupiravir in EtOAc at 20 °C has a steep dependence on the water content, with a solubility of 40 mg/mL at 3 wt % water but only 5 mg/mL at 0.5 wt %. In the original process, the API crystallizes during the azeotropic distillation operation, which can lead to variability across different equipment trains and scales that can impact purity and physical attributes such as particle size distribution and bulk density. Thus, we modified the azeotropic distillation/crystallization process into distinct steps in which the API would crystallize under controlled conditions that are less sensitive to variations in equipment and scales.

In order to crystallize the product, the ethyl acetate solution is azeotropically dried to approximately 4.0 wt % water and 80 mg/mL concentration, followed by seeding. At this point, dry EtOAc is added slowly, which acts to further decrease the overall water content to 2.5 wt % and the solubility of molnupiravir to approximately 25 mg/mL. The crystallization of the majority of the API during the slow addition of EtOAc offers more control compared to crystallization during the distillation operation and was found to reliably afford high-purity API with consistent physical properties across several sites and equipment trains. Finally, the solution is further concentrated to a final target of 4 L/kg and ≤1 wt % water, and 4 L/kg of MTBE is added to aid in product recovery. Crystalline molnupiravir is isolated by filtration and washing, with an overall isolated yield of 76% and HPLC purity >99.5%. Compared to the original process, the revised reaction and isolation conditions are inherently robust and ensure that high-purity API with consistent physical attributes is reliably isolated across our many different manufacturing sites.

In conclusion, we have improved the yields, robustness, cycle times, and overall throughput for each of the five steps in the synthesis of molnupiravir from uridine (Scheme 9). The overall yield was improved by 1.6-fold compared to the original process (57 vs 36%), and this revised process is being used to prepare molnupiravir at a rate of over 100 metric tons per year across several manufacturing sites. Our investments in process improvements ensure the most rapid conversion of uridine to high-purity molnupiravir at metric ton scales and prevent several million kilograms of waste per year.

■ ASSOCIATED CONTENT

Supporting Information

The Supporting Information is available free of charge at https://pubs.acs.org/doi/10.1021/acs.oprd.1c00400.

Experimental procedures and characterization data (PDF)

■ AUTHOR INFORMATION

Corresponding Authors

Patrick S. Fier − *Department of Process Research and Development, Merck & Co., Inc., Rahway, New Jersey 07065, United States;* orcid.org/0000-0002-6102-815X; Email: patrick.fier@merck.com

Yingju Xu − *Department of Process Research and Development, Merck & Co., Inc., Rahway, New Jersey 07065, United States*; Email: yingju_xu@merck.com

Authors

Marc Poirier − *Department of Process Research and Development, Merck & Co., Inc., Rahway, New Jersey 07065, United States*

Gilmar Brito − *Department of Process Research and Development, Merck & Co., Inc., Rahway, New Jersey 07065, United States*

Michelle Zheng − *Department of Process Research and Development, Merck & Co., Inc., Rahway, New Jersey 07065, United States*

Rachel Bade − *Department of Process Research and Development, Merck & Co., Inc., Rahway, New Jersey 07065, United States;* orcid.org/0000-0002-5384-9687

Eric Sirota − *Department of Process Research and Development, Merck & Co., Inc., Rahway, New Jersey 07065, United States;* orcid.org/0000-0002-6205-0295

Kevin Stone − *Department of Process Research and Development, Merck & Co., Inc., Rahway, New Jersey 07065, United States*

Lushi Tan − *Department of Process Research and Development, Merck & Co., Inc., Rahway, New Jersey 07065, United States*

Guy R. Humphrey − *Department of Process Research and Development, Merck & Co., Inc., Rahway, New Jersey 07065, United States;* orcid.org/0000-0001-8634-1567
Darryl Chang − *Department of Process Research and Development, Merck & Co., Inc., Rahway, New Jersey 07065, United States*
Jameson Bothe − *Department of Process Research and Development, Merck & Co., Inc., Rahway, New Jersey 07065, United States*
Yongqian Zhang − *Department of Process Research and Development, Merck & Co., Inc., Rahway, New Jersey 07065, United States*
Frank Bernardoni − *Department of Process Research and Development, Merck & Co., Inc., Rahway, New Jersey 07065, United States*
Steve Castro − *Department of Process Research and Development, Merck & Co., Inc., Rahway, New Jersey 07065, United States*
Michael A. Zompa − *Department of Process Research and Development, Merck & Co., Inc., Rahway, New Jersey 07065, United States;* orcid.org/0000-0003-2401-7846
Jerry Taylor − *Department of Process Research and Development, Merck & Co., Inc., Rahway, New Jersey 07065, United States*
Kevin M. Sirk − *Department of Process Research and Development, Merck & Co., Inc., Rahway, New Jersey 07065, United States*
Anthony Diaz-Santana − *Department of Process Research and Development, Merck & Co., Inc., Rahway, New Jersey 07065, United States*
Ike Diribe − *Department of Process Research and Development, Merck & Co., Inc., Rahway, New Jersey 07065, United States*
Khateeta M. Emerson − *Department of Process Research and Development, Merck & Co., Inc., Rahway, New Jersey 07065, United States;* orcid.org/0000-0001-9226-2152
Bharath Krishnamurthi − *Department of Process Research and Development, Merck & Co., Inc., Rahway, New Jersey 07065, United States*
Ralph Zhao − *Department of Process Research and Development, Merck & Co., Inc., Rahway, New Jersey 07065, United States;* orcid.org/0000-0003-2205-8919
Michael Ward − *Department of Process Research and Development, Merck & Co., Inc., Rahway, New Jersey 07065, United States*
Chengqian Xiao − *WuXi AppTec Co., Ltd., Shanghai 200131, China*
Honggui Ouyand − *WuXi AppTec Co., Ltd., Shanghai 200131, China*
Jianfeng Zhan − *WuXi AppTec Co., Ltd., Shanghai 200131, China*
William J. Morris − *Department of Process Research and Development, Merck & Co., Inc., Rahway, New Jersey 07065, United States;* orcid.org/0000-0003-4322-4509

Complete contact information is available at: https://pubs.acs.org/10.1021/acs.oprd.1c00400

Notes

The authors declare no competing financial interest.

■ ACKNOWLEDGMENTS

We would like to thank our colleagues Lisa Jellett, Plamen Grigorov, Elizabeth Fisher, Noel Dinan, and Kevin Maloney for helpful discussion. We would like to thank Lauren Weisel, Srinivas Tekkam (Merck & Co., Inc., Rahway, NJ, USA), Guiquan Liu, Baoqiang Wan, Yanpei Yu, Yimei Wan, Ziheng Wang, Ling Ran, Ning Gao, Qiyi Wang, Yingqian Han, Liangtao Zhu, Lipeng Zhang, Kunhai Tang, and Wanyong Fu (Wuxi AppTec Co., China) for technical support.

■ REFERENCES

(1) Merck and Ridgeback Bio Collaborate to Advance Development of Novel Antiviral Candidate, EIDD-2801. https://www.businesswire.com/news/home/20200526005229/en/ (Accessed October 25, 2021).
(2) Cox, R. M.; Wolf, J. D.; Plemper, R. K. Therapeutically administered ribonucleoside analogue MK-4482/EIDD-2801 blocks SARS-CoV-2 transmission in ferrets. *Nat. Microbiol.* **2021**, *6*, 11−18.
(3) Sheahan, T. P.; Sims, A. C.; Zhou, S.; Graham, R. L.; Pruijssers, A. J.; Agostini, M. L.; Leist, S. R.; Schäfer, A.; Dinnon, K. H., III; Stevens, L. J.; Chappell, J. D.; Lu, X.; Hughes, T. M.; George, A. S.; Hill, C. S.; Montgomery, S. A.; Brown, A. J.; Bluemling, G. R.; Natchus, M. G.; Saindane, M.; Kolykhalov, A. A.; Painter, G.; Harcourt, J.; Tamin, A.; Thornburg, N. J.; Swanstrom, R.; Denison, M. R.; Baric, R. S. An orally bioavailable broad-spectrum antiviral inhibits SARS-CoV-2 in human airway epithelial cell cultures and multiple coronaviruses in mice. *Sci. Transl. Med.* **2020**, *12*, No. eabb5883.
(4) Wahl, A.; Gralinski, L. E.; Johnson, C. E.; Yao, W.; Kovarova, M.; Dinnon, K. H.; Liu, H.; Madden, V. J.; Krzystek, H. M.; De, C.; White, K. K.; Gully, K.; Schäfer, A.; Zaman, T.; Leist, S. R.; Grant, P. O.; Bluemling, G. R.; Kolykhalov, A. A.; Natchus, M. G.; Askin, F. B.; Painter, G.; Browne, E. P.; Jones, C. D.; Pickles, R. J.; Baric, R. S.; Garcia, J. V. SARS-CoV-2 infection is effectively treated and prevented by EIDD-2801. *Nature* **2021**, *591*, 451.
(5) *Merck and Ridgeback's Investigational Oral Antiviral Molnupiravir Reduced the Risk of Hospitalization or Death by Approximately 50 Percent Compared to Placebo for Patients with Mild or Moderate COVID-19 in Positive Interim Analysis of Phase 3 Study*; Press Release from Merck & Co., Inc., 2021. Oct 1st.
(6) Kabinger, F.; Stiller, C.; Schmitzová, J.; Dienemann, C.; Kokic, G.; Hillen, H. S.; Höbartner, C.; Cramer, P. Mechanism of molnupiravir-induced SARS-CoV-2 mutagenesis. *Nat. Struct. Mol. Biol.* **2021**, *28*, 740.
(7) For selected lab-scale syntheses of MK-4482, see: (a) Painter, G. R.; Bluemling, G. R.; Natchus, M. G.; Guthrie, D. N4-Hydroxycytidine and Derivatives and Anti-Viral Uses Related Thereto. WO2019113462, 2018. (b) Painter, G. R.; Perryman, D.; Bluemling, G. R. 4'-Halogen Containing Nucleotide and Nucleoside Therapeutic Compositions and Uses Related Therto. WO2019173602, 2019. (c) Vasudevan, N.; Ahlqvist, G. P.; McGeough, C. P.; Paymode, D. J.; Cardoso, F. S. P.; Lucas, T.; Dietz, J.-P.; Opatz, T.; Jamison, T. F.; Gupton, F. B.; Snead, D. R. A concise route to MK-4482 (EIDD-2801) from cytidine. *Chem. Commun.* **2020**, *56*, 13363. (d) Paymode, D. J.; Vasudevan, N.; Ahmad, S.; Kadam, A. L.; Cardoso, F. S. P.; Burns, J. M.; Cook, D. W.; Stringham, R. W.; Snead, D. R. Toward a Practical, Two-Step Process for Molnupiravir: Direct Hydroxamination of Cytidine Followed by Selective Esterification. *Org. Process Res. Dev.* **2021**, *25*, 1822.
(8) Clode, D. M. Carbohydrate cyclic acetal formation and migration. *Chem. Rev.* **1979**, *79*, 491.
(9) (a) Abdel Rahman, A. A.-H.; Wada, T.; Saigo, K. Facile Methods for the Synthesis of 5-Formylcytidine. *Tetrahedron Lett.* **2001**, *42*, 1061. (b) Divakar, K. J.; Reese, C. B. 4- (1,2,4-Triazol-1-yl)- and 4-(3-Nitro-1,2,4-triazol-1-yl)-1 -(β-D-2,3,5-tri-O-acetylarabinofuranosyl)-pyrimidin-2(1H)-ones. Valuable Intermediates in the Synthesis of

Derivatives of 1 -(β -D-Arabinofuranosy1)cytosine (Ara-C). *J. Chem. Soc., Perkin Trans.* **1982**, *1*, 1171. (c) Gao, Y.; Zhang, P.; Wu, L.; Matsuura, T.; Meng, J. Synthesis of Uridine Derivatives Containing Amino Acid Residues. *Synth. Commun.* **2003**, *33*, 2635.

(10) (a) Sasidharan, N.; Hariharanath, B.; Rajendran, A. G. Thermal Decomposition Studies on Energetic Triazole Compounds. *Thermochim. Acta* **2011**, *520*, 139.

(11) Webb, T. R.; Mitsuya, H.; Broder, S. 1-(2,3-Anhydro-β-D-lyxofuranosyl)cytosine Derivatives as Potential Inhibitors of the Human Immunodeficiency Virus. *J. Med. Chem.* **1988**, *31*, 1475.

(12) U.S. Chemical Safety and Hazard Investigation Board. *The Explosion at Concept Sciences: Hazards of Hydroxylamine*, 2002. No. 1999-13-C-PA.

https://doi.org/10.1021/acs.oprd.1c00400
Org. Process Res. Dev. 2021, 25, 2806−2815